

# Appendices

## Appendix A. Subtour elimination constraints

### Appendix A.1. Subtours in the Traveling Salesman Problem

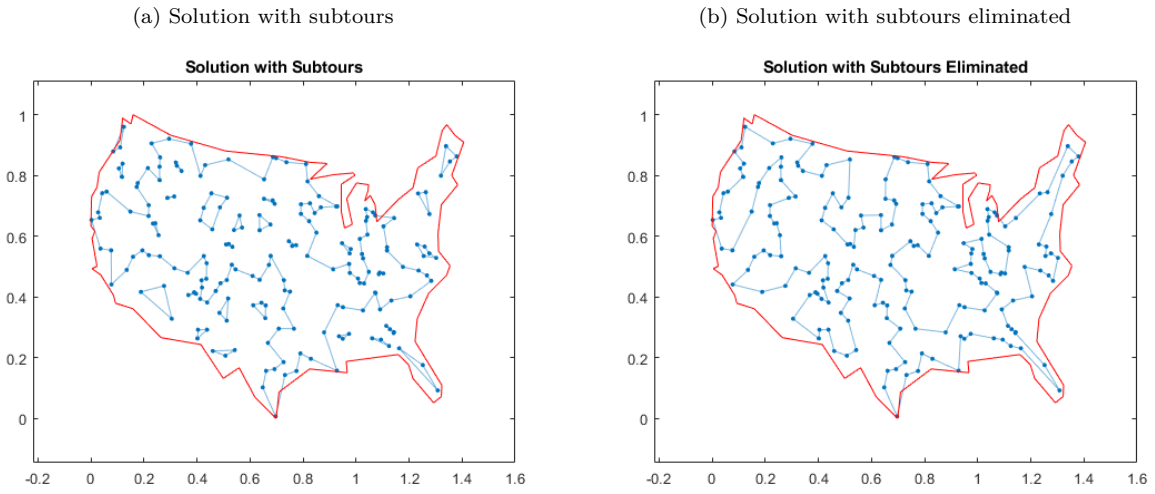


Figure A.1: Example of subtours from Traveling Salesman Problem: Problem-Based (MathWorks, 2021)

### Appendix A.2. Subtours elimination constraints in the orienteering problem

For every subset of nodes (port excluded), the number of visited edges inside the subset ( $x_{ij}$ -values equal to 1) should be strictly smaller than the number of nodes in the subset. Since not all nodes are visited in the solution of the orienteering problem, Feillet et al. (2005) defined the subtour elimination constraints as in Equation A.1. The bidirectional setting of  $x_{ij}$  naturally deletes subtours with only two nodes.<sup>27</sup> Number of nodes within the subset  $S$  is  $|S| = \sum_{i \in S} y_i$ , where  $S$  does not include the port ( $S \subset \{2, \dots, N\}$ ).

$$\sum_{i,j \in S: i \neq j} x_{ij} \leq \sum_{i \in S \setminus \{k\}} y_i; \forall S \subset \{2, \dots, N\}, |S| \geq 3, k \in S. \quad (\text{A.1})$$

---

<sup>27</sup>A subtour of two nodes  $i$  and  $j$  requires both  $x_{ij} = 1$  and  $x_{ji} = 1$ . But the bidirectional edge  $x_{ij} = 1$  represents either the edge from  $i$  to  $j$  is taken or the edge of  $j$  to  $i$  is taken but not both. Therefore there are no subtours of two nodes with the bidirectional edge  $x_{ij}$ .

$k$  is an arbitrary node in the subset  $S$ .  $\sum_{i \in S \setminus \{k\}} y_i$  is the sum of chosen nodes within  $S$  excluding Node  $k$ .

To illustrate how the constraints work in Equation A.1, we use  $N = 5$  as an example of the subtour elimination constraints. With 5 nodes in total and Node 1 as the port, subsets of nodes excluding the port  $S \subset N \setminus \{1\} = \{2, 3, 4, 5\}$ . The setting of undirected  $x_{ij}$  naturally deleted subtours with only two nodes. So the possible subtours will either include 3 nodes or 4 nodes. There will be  $C_4^3 + C_4^4 = 5$  possible subtours.

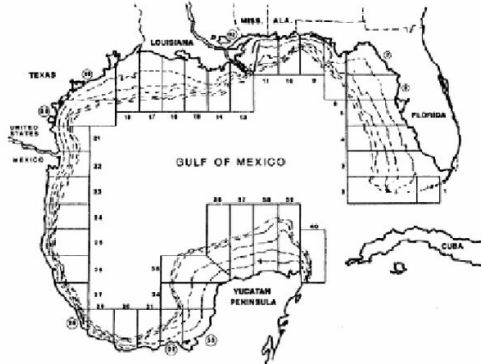
$$\{2, 3, 4\}, \{2, 3, 5\}, \{2, 4, 5\}, \{3, 4, 5\}, \{2, 3, 4, 5\}.$$

Here we arbitrarily exclude the last column to obtain  $\sum_{i \in S \setminus \{k\}} y_i$  ( $k \in S$  is visited). The results are the same with any column in  $S$  excluded. So the subtour elimination constraints in Equation A.1 will be:

$$\begin{aligned} x_{23} + x_{24} + x_{34} &\leq y_2 + y_3 \\ x_{23} + x_{25} + x_{35} &\leq y_2 + y_3 \\ x_{24} + x_{25} + x_{45} &\leq y_2 + y_4 \\ x_{34} + x_{35} + x_{45} &\leq y_3 + y_4 \\ x_{23} + x_{24} + x_{25} + x_{34} + x_{35} + x_{45} &\leq y_2 + y_3 + y_4. \end{aligned} \tag{A.2}$$

## Appendix B. The Gulf of Mexico longline fleet

(a) Trip-level logbook data



(b) Fishing heatmap using hourly VMS data

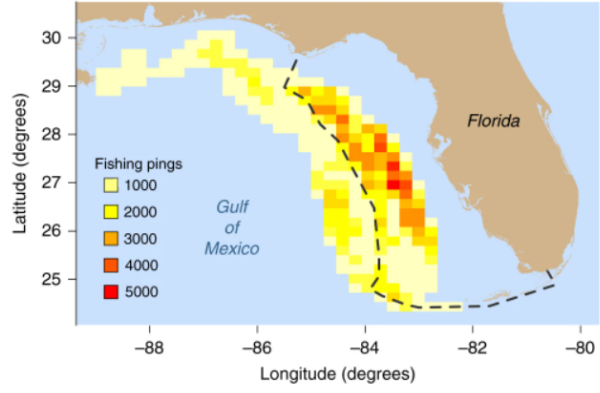


Figure B.1: Historical and contemporary data of longline fishing in the Gulf of Mexico. Figure B.1a from (Cass-Calay, 2013) shows the statistical areas used by the U.S. National Marine Fisheries Service (NMFS) trip-level logbook reporting. Figure B.1b is a heatmap of fishing activity by longline vessels using the hourly Vessel Monitoring System (VMS) positions. Source for Figure B.1b is O'Farrell et al. (2019b).

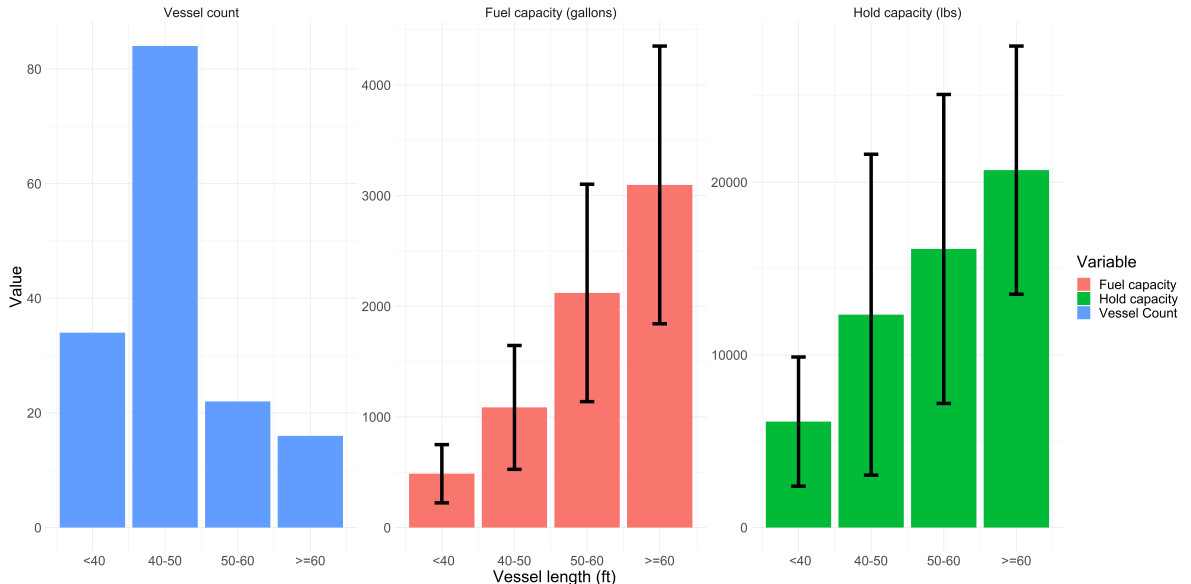


Figure B.2: Fuel, hold capacity, and vessel count for vessel groups based on length in the Gulf of Mexico Longline fisheries. Errorbar shows the standard deviation within the length group. Source: Fishery logbook data from 2005 to 2012.

## Appendix C. Solution method and optimality conditions

### Appendix C.1. Pseudo algorithm

- Step 1. Initial Optimization: We find a solution on nodes, edges, and effort generated by Gurobi. Gurobi generates the first guess for the algorithm (see below), and the solution is within the tolerance  $10^{-4}$ .
- Step 2. First-order condition analysis: We take the optimal solution from step 1 and verify whether the solution satisfies the first-order condition and binding technology constraint. If it violates these conditions, we identify potential improvements in effort distribution in step 3.
- Step 3. Effort reallocation: Based on our findings in step 2, we use the nodes and edges from the solution in step 1 to derive the optimal effort allocation and shadow prices of the technology constraints using both the binding technology constraint and first-order conditions directly.
- Step 4. Solution refinement: We then use the reallocated effort, nodes, and edges found in step 3 as an initial guess and resolve the optimization problem in Gurobi. We report the solution when the solver confirms this initial guess.

### Appendix C.2. Gurobi branch-and-bound algorithm

Gurobi solves the MIP maximization problem starting with an initial relaxation where binary variables  $x_{ij}$  and  $y_i$  are treated as continuous between 0 and 1, which provides an upper bound (best bound) on the objective function. This initial solution may contain fractional values. If the relaxed solution is not integer, branching occurs: Gurobi selects a fractional variable and creates two subproblems—one fixing the variable to 0 (not chosen) and one to 1 (chosen). This branching forms a decision tree about which sites to select and which paths to include.

For each branch, bounding is applied by solving a relaxed version of the subproblem to estimate the best possible solution within that branch. If this bound is worse than the current best feasible solution, the branch is pruned. Additionally, hold capacity constraints and fuel constraints are checked for feasibility.

During this process, Gurobi tracks the best feasible solution found (lower bound/best integer). If a subproblem yields an integer solution that improves the current best, the lower bound is updated. When the relative difference between the lower and upper bounds ( $|upper bound - lower bound|/(|lower bound|)$ ) becomes less than the MIP gap tolerance (default  $10^{-4}$ ), Gurobi terminates and returns this solution as optimal or near-optimal.

### *Appendix C.3. Optimal unconstrained and constrained fishing hour*

If the initial solution from Section Appendix C.2 for fishing effort does not satisfy the optimality conditions in Table 2, then we modify the solution to ensure that it does satisfy them. To obtain a solution consistent with economic theory, we derive the optimal fishing hours  $A_i^*$  and the corresponding fishing effort  $A_i\eta$  following the conditions (detailed derivation steps are provided below). We then use these theoretically-derived values as an initial guess to resolve the optimization problem, resulting in a higher objective function value that satisfies the effort allocation principle.

The Lagrange function of the forward-looking fisher optimization problem (Problem 1) is

$$\begin{aligned} \mathcal{L}(x_{ij}, y_i, A_i, \lambda) = & \sum_{i \in N} (pqA_i^\gamma \eta^\gamma Stock_i y_i - c_{fuel}af\eta\kappa A_i) - \sum_{(i,j) \in E} d_{ij}x_{ij}bf c_{fuel} \\ & - \lambda_{fuel}(\sum_{(i,j) \in E} d_{ij}x_{ij}bf + \sum_{(i) \in N} A_i af\eta\kappa - F_{max}) \\ & - \lambda_{hold}(\sum_{i \in N} qA_i^\gamma \eta^\gamma Stock_i y_i - C_{max}). \end{aligned} \quad (C.1)$$

The first order condition of fishing hour  $A_i$  at each site is

$$\begin{aligned}\partial\mathcal{L}/\partial A_i &= pq\text{Stock}_i y_i \gamma A_i^{\gamma-1} \eta^\gamma - c_{fuel} af \eta \kappa - \lambda_{fuel} af \eta \kappa - \lambda_{hold} q \text{Stock}_i y_i \gamma A_i^{\gamma-1} \eta^\gamma \\ &= (p - \lambda_{hold}) q \text{Stock}_i y_i \gamma A_i^{\gamma-1} \eta^\gamma - (c_{fuel} + \lambda_{fuel}) af \eta \kappa = 0 \\ \Rightarrow A_i^* &= \left( \frac{(p - \lambda_{hold}) q \text{Stock}_i y_i \gamma \eta^\gamma}{(c_{fuel} + \lambda_{fuel}) af \eta \kappa} \right)^{\frac{1}{1-\gamma}}.\end{aligned}\quad (\text{C.2})$$

1. If neither fuel nor hold constraint binds ( $\lambda_{fuel} = \lambda_{hold} = 0$ ),  $A_i^* = \left( \frac{pq\text{Stock}_i y_i \gamma \eta^\gamma}{c_{fuel} af \eta \kappa} \right)^{\frac{1}{1-\gamma}}$ .
2. If the fuel constraint binds while hold constraint doesn't.  $\lambda_{fuel} > 0, \lambda_{hold} = 0$ . From the FOC, we can derive  $A_i^*(\lambda_{fuel})$ , the optimal fishing hour as a function of  $\lambda_{fuel}$ .

$$\begin{aligned}A_i^* &= \left( \frac{(p - \lambda_{hold}) q \text{Stock}_i y_i \gamma \eta^\gamma}{(c_{fuel} + \lambda_{fuel}) af \eta \kappa} \right)^{\frac{1}{1-\gamma}} \\ &= \left( \frac{pq\text{Stock}_i y_i \gamma \eta^\gamma}{(c_{fuel} + \lambda_{fuel}) af \eta \kappa} \right)^{\frac{1}{1-\gamma}}.\end{aligned}\quad (\text{C.3})$$

Use the binding fuel constraint, we can solve  $\lambda_{fuel}$  and therefore  $A_i^*$ .

$$\begin{aligned}\sum_{(i,j) \in E} d_{ij} x_{ij} bf + \sum_{(i) \in N} A_i af \eta \kappa &= F_{max} \\ \Rightarrow \sum_{(i,j) \in E} d_{ij} x_{ij} bf + \sum_{(i) \in N} \left( \frac{pq\text{Stock}_i y_i \gamma \eta^\gamma}{(c_{fuel} + \lambda_{fuel}) af \eta \kappa} \right)^{\frac{1}{1-\gamma}} af \eta \kappa &= F_{max} \\ \Rightarrow \lambda_{fuel} &\\ \Rightarrow A_i^* &= \left( \frac{pq\text{Stock}_i y_i \gamma \eta^\gamma}{(c_{fuel} + \lambda_{fuel}) af \eta \kappa} \right)^{\frac{1}{1-\gamma}} \text{ using derived } \lambda_{fuel}.\end{aligned}\quad (\text{C.4})$$

3. If the fuel constraint doesn't bind while the hold constraint binds,  $\lambda_{fuel} = 0, \lambda_{hold} > 0$ .

Similarly, we can derive  $A_i^*(\lambda_{hold})$  from the FOC, the optimal fishing hour as a function of  $\lambda_{hold}$ .

$$\begin{aligned}A_i^* &= \left( \frac{(p - \lambda_{hold}) q \text{Stock}_i y_i \gamma \eta^\gamma}{(c_{fuel} + \lambda_{fuel}) af \eta \kappa} \right)^{\frac{1}{1-\gamma}} \\ &= \left( \frac{(p - \lambda_{hold}) q \text{Stock}_i y_i \gamma \eta^\gamma}{c_{fuel} af \eta \kappa} \right)^{\frac{1}{1-\gamma}}.\end{aligned}\quad (\text{C.5})$$

Using the binding hold constraint, we can solve  $\lambda_{hold}$  and therefore  $A_i^*$ .

$$\begin{aligned}
\sum_{i \in N} q A_i^\gamma \eta^\gamma Stock_i y_i &= C_{max} \\
\Rightarrow \sum_{i \in N} q \left( \frac{(p - \lambda_{hold}) q Stock_i y_i \gamma \eta^\gamma}{c_{fuel} a f \eta \kappa} \right)^{\frac{1}{1-\gamma}} \eta^\gamma Stock_i y_i &= C_{max} \\
&\Rightarrow \lambda_{hold} \\
\Rightarrow A_i^* &= \left( \frac{(p - \lambda_{hold}) q Stock_i y_i \gamma \eta^\gamma}{c_{fuel} a f \eta \kappa} \right)^{\frac{1}{1-\gamma}} \text{ using derived } \lambda_{hold}.
\end{aligned} \tag{C.6}$$

#### Appendix C.4. Shadow price of fuel

The vessel-trip-specific shadow price of fuel  $\lambda_{fuel}$  is influenced by the economic value of the ecosystem. System productivity is primarily determined by fish stock abundance, whereas the number and spatial arrangement of fishing sites affect the efficiency with which vessels operate. Higher total fish stock abundance increases the system's potential revenue, thereby influencing the relative value of fuel. The spatial distribution of fishing sites influences fuel consumption for both travel and fishing. For example, in a system with more dispersed sites, fishers may spend more fuel on travelling and less on fishing. This leads to lower fishing effort at each location and consequently a higher shadow price of fuel. While the number of sites may not always affect total fish stock, it does impact inter-site distances and overall fuel efficiency. These factors can thus alter the shadow price of fuel, which represents its marginal value in terms of system productivity.

Table C.1: Factors affecting the shadow price of fuel ( $\lambda_{fuel}$ ) for fishing vessels

Category	Factors	Effect on $\lambda_{fuel}$ as factor increases
Vessel characteristics	Fuel constraint $F_{max}$	↓
	Degree of forward-looking	↑
Economic factors	Fish price ( $p$ )	↑
	Effort output elasticity ( $\gamma$ )	↓
	Fishing fuel efficiency multiplier ( $\kappa$ )	↓
Environmental and spatial factors	Total Fish stock abundance	↑
	Number of fishing sites	?
	Spatial distribution of sites ( $d_{ij}$ )	↑ for more dispersed sites

## Appendix D. Parameter values used in simulation

Table D.1: Parameter values used in the simulation

Parameters	description	Value	Source
N	the set of nodes in the network (the port and fishing sites)	15	assumed
E	the set of edges in the network	$C_{15}^2$	
$d_{ij}$	travel distance in nm between node $i$ and $j$ . $d_{ij} = d_{ji}$ in the undirected case		calculated based on coordinates
Stock <sub>i</sub>	fish stock at node $i$	calibrated <sup>1</sup>	
p	ex-vessel price \$ per lb	3	fishery logbook data <sup>2</sup>
$c_{fuel}$	\$ per gallon, unit cost of fuel usage	2	fishery logbook data <sup>3</sup>
q	catchability coefficient	$1.55 \times 10^{-5}$	derived <sup>4</sup>
f	fuel usage, gallon per hour	5	assumed <sup>5</sup>
a	fishing effort fuel consumption coefficient	0.001	$a\eta = 1$
speed	traveling speed, knots (nautical mile per hour)	5	assumed <sup>5</sup>
b	traveling fuel consumption coefficient, 1/speed,	0.2	
$\gamma$	output elasticity of fishing effort	0.7	<1 (Zhang and Smith, 2011) <sup>6</sup>
$\beta$	output elasticity of fish stock	1	Zhang and Smith (2011)
$\eta$	hook number for longline	1000	NOAA regulations <sup>7</sup>
$\kappa$	fishing fuel consumption is $\kappa$ times as large as traveling	2	assumed

<sup>1</sup> Stock is calibrated such that the fishing hours at each site, trip length, and total catch per trip align with the average or midpoint values recorded in the logbook data. In the study by (Dépalle et al., 2021), the average days at sea per trip for the Gulf of Mexico Reef Fish fishery's bottom longline fleet was found to be approximately 7.5 days in 2005. This increased to an annual average of 10 days between 2008 and 2012. Additionally, the pounds landed amounted to 3,779 pounds in 2008 and rose to 6,312 pounds in 2012.

<sup>2</sup> (Dépalle et al., 2021) reports inflation-adjusted revenues as \$12,300 for 3,779 pounds in 2008 and \$21,911 for 6,312 pounds in 2012. This translates to an average price per pound of approximately \$3.25 in 2008, rising to about \$3.47 in 2012.

<sup>3</sup> Diesel price  $c_{fuel} \in [0.95, 4.75]$  with mean 2.5 and median 2.67.

<sup>4</sup> See derivation in Appendix Section Appendix D.1.

<sup>5</sup> Lian (2012) surveyed West Coast open access groundfish and salmon troll fisheries. The average vessel speed is 3.8 knots when longlining while the average fuel use is 2 gallons per hour when longlining. However, those vessels are relatively smaller because the average crew size is 1.5. While the average crew size is 3.1 for GoM bottom longline vessels.

<sup>6</sup> The estimated catch effort elasticity for bottom longline is 0.3325 with standard error 0.0093 in Zhang and Smith (2011). However, the effort in Zhang and Smith (2011) is defined as the number of crew times trip days while the effort in this paper is defined as the number of hooks times fishing hours (longline set, soak and retrieve time).

<sup>7</sup> The 1,000 hooks per vessel limit onboard commercial reef fish bottom longline vessels was removed in 2018 (NOAA, 2018).

### Appendix D.1. Derivation of catchability coefficient q

The catchability coefficient  $q$  is chosen so that the unconstrained optimal harvest at each site is interior  $q(A_i^*)^\gamma \text{Stock}_i y_i \eta^\gamma < \text{Stock}_i$ . With no constraint on fuel and hold,  $\lambda_{fuel} = \lambda_{hold} = 0$ .

$$\begin{aligned}
 A_i^* &= \left( \frac{(p - \lambda_{hold})q \text{Stock}_i y_i \gamma \eta^\gamma}{(c_{fuel} + \lambda_{fuel})af \eta \kappa} \right)^{\frac{1}{1-\gamma}} \\
 &= \left( \frac{pq \text{Stock}_i y_i \gamma \eta^\gamma}{c_{fuel} af \eta \kappa} \right)^{\frac{1}{1-\gamma}} \\
 &= \left( \frac{pq \text{Stock}_i y_i \gamma}{c_{fuel} af \eta^{1-\gamma} \kappa} \right)^{\frac{1}{1-\gamma}}.
 \end{aligned} \tag{D.1}$$

The unconstrained optimal harvest at each site should not exceed the available stock.

$$\begin{aligned}
q(A_i^*)^\gamma \text{Stock}_i y_i \eta^\gamma &< \text{Stock}_i \\
q(A_i^*)^\gamma y_i \eta^\gamma &< 1 \\
qy_i \left( \frac{pq\text{Stock}_i y_i \gamma \eta^\gamma}{c_{fuel}af\eta\kappa} \right)^{\frac{1}{1-\gamma}} \eta^\gamma &< 1 \\
q^{\frac{1}{1-\gamma}} y_i^{\frac{1}{1-\gamma}} \left( \frac{p\text{Stock}_i \gamma \eta^\gamma}{c_{fuel}af\eta\kappa} \right)^{\frac{1}{1-\gamma}} \eta^\gamma &< 1 \\
q^{\frac{1}{1-\gamma}} y_i^{\frac{1}{1-\gamma}} &< \left( \frac{p\text{Stock}_i \gamma}{c_{fuel}af\kappa} \right)^{\frac{1}{1-\gamma}} \\
qy_i &< \left( \frac{c_{fuel}af\kappa}{p\text{Stock}_i \gamma} \right)^\gamma.
\end{aligned} \tag{D.2}$$

Given parameter values of  $\{\text{Stock}_i, a, p, c_{fuel}, q, \eta, \kappa\}$  is chosen so that works for all site,

$$qy_i = \frac{1}{2} \min \left[ \left( \frac{c_{fuel}af\kappa}{p\text{Stock}_i \gamma} \right)^\gamma \right].$$

## Appendix E. Sensitivity Analysis

### Appendix E.1. Results for random pattern of fish stocks

The first sensitivity analysis involves distributing the stock randomly across the same 14 fishing sites. This analysis highlights how vessels choose site, effort, and route when the spatial structure of the stock is absent, which is a case where the forward-looking and myopic fisher solutions could potentially differ more than in the base case. The absence of a clear stock spatial structure might lead to increased distances to high-stock sites and amplify the inefficiency of the myopic fisher. The myopic fisher without route planning, may end up expending more fuel which constrains both the number of sites to visit and the effort allocated at these fishing sites.

### Appendix E.2. Results for clustered fishing sites

The second sensitivity analysis focuses on adjusting the spatial proximity of the sites, making them more clustered. The stock distribution exhibits a spatial pattern in which higher stock levels are found at the nearshore sites. By grouping these sites closer together,

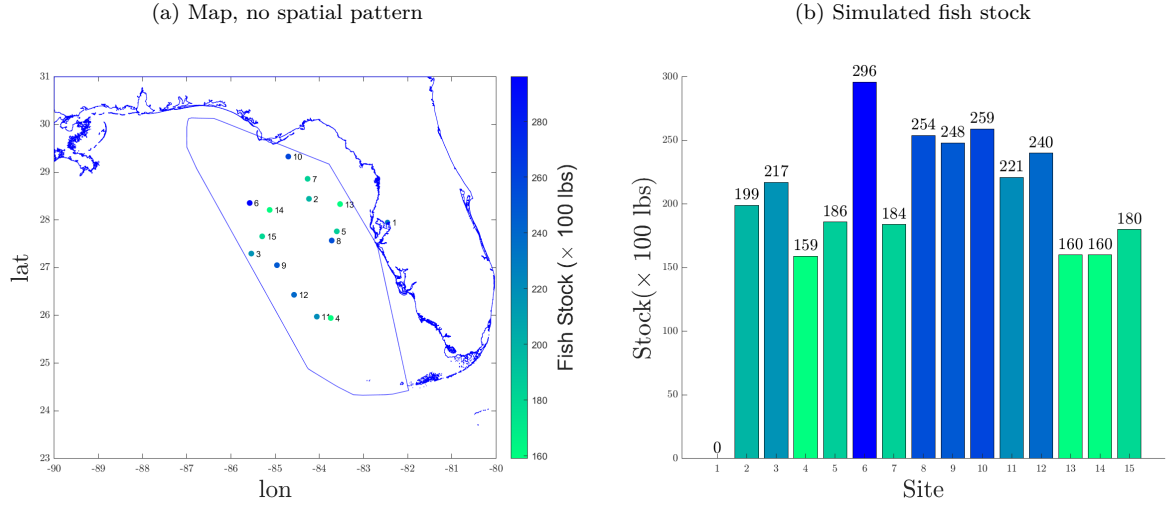


Figure E.1.1: Spatial distribution and fish stock of the port (Node 1) and 14 fishing sites in the Gulf of Mexico.

Table E.1.1: Fuel and Hold Usage, Binding Constraints, Shadow Price, Travel Route and Time

Variable	Unconstrained		Fuel		Hold	
	$F_{max} = 20,000, C_{max} = 20,000$	$F_{max} = 3,000, C_{max} = 20,000$	$F_{max} = 3,000, C_{max} = 20,000$	$F_{max} = 20,000, C_{max} = 3,000$	$F_{max} = 20,000, C_{max} = 3,000$	$F_{max} = 20,000, C_{max} = 3,000$
Vessel Type	Forward-looking	Myopic	Forward-looking	Myopic	Forward-looking	Myopic
Profit	0.892 $\pi_{\text{forward-looking}}$		0.32 $\pi_{\text{forward-looking}}$		0.449 $\pi_{\text{forward-looking}}$	
Fuel Usage	16916	17606	3000	3000	2183.9	3461.1
Harvest/100	155.15	155.15	40.296	26.525	30	30
Shadow price	-		$\lambda_{\text{fuel}} = 1.5641$		$\lambda_{\text{hold}} = 143.32$	
Travel%	7.1%	13.9%	34.5%	20%	39.6%	17.6%
Fishing%	92.9%	86.1%	65.5%	79.97%	60.4%	82.4%
Trip Length (days)	73.091	78.838	15.107	13.891	11.345	15.815

<sup>1</sup> Travel% denotes percentage of travel time of the total trip length. Same for Fishing%.

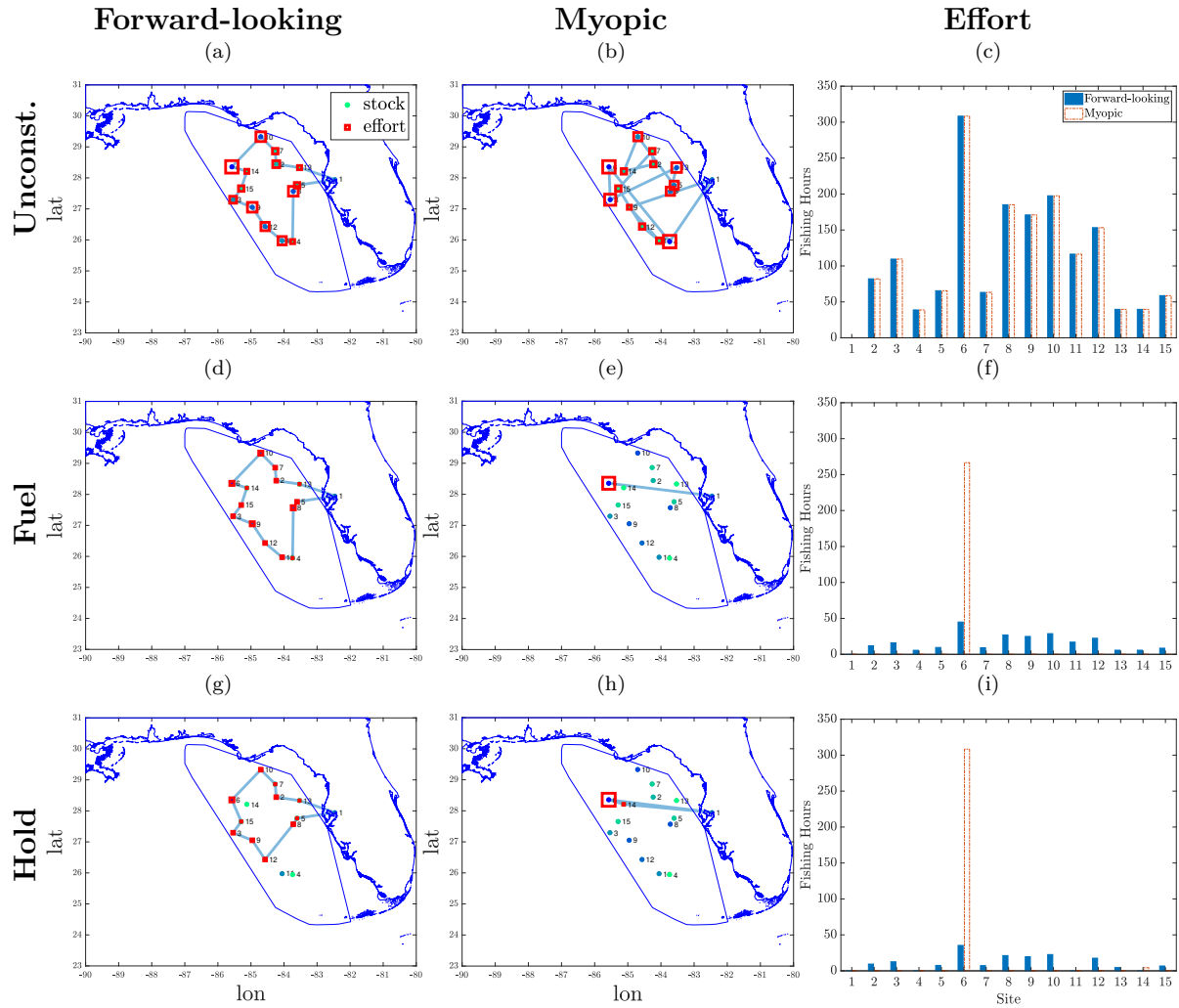


Figure E.1.2: Simulated travel path and fishing effort, forward-looking vessel vs myopic vessel, with random stock distribution.

this analysis can examine how changes in spatial density or clustering might influence fishing decision-making. We expect to see less difference between the forward-looking and myopic fishers because the inefficiencies due to travel and site choice are smaller, everything else being equal.

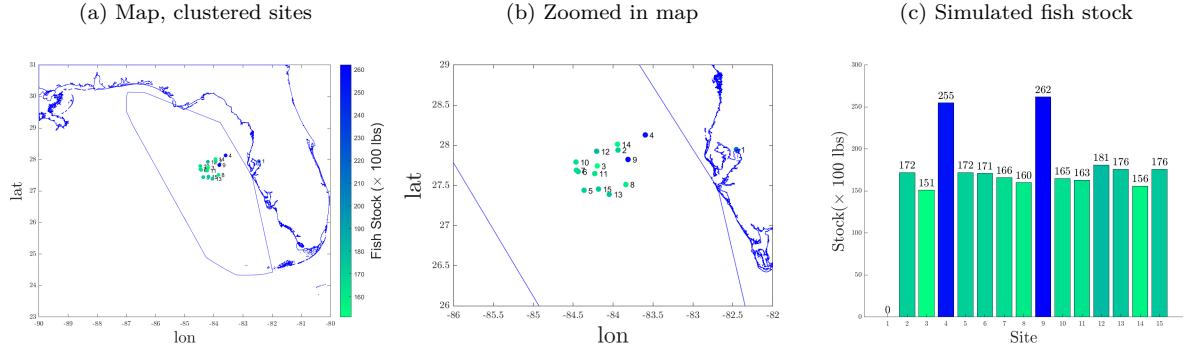


Figure E.2.1: Spatial distribution and fish stock of the port (Node 1) and 14 fishing sites in the Gulf of Mexico.

Table E.2.1: Fuel and Hold Usage, Binding Constraints, Shadow Price, Travel Route and Time

Variable	Unconstrained		Fuel		Hold	
	$F_{max} = 20,000, C_{max} = 20,000$	Forward-looking	$F_{max} = 3,000, C_{max} = 20,000$	Myopic	$F_{max} = 20,000, C_{max} = 3,000$	Forward-looking
Vessel Type	Forward-looking	Myopic	Forward-looking	Myopic	Forward-looking	Myopic
Profit	0.967 $\pi_{\text{forward-looking}}$			0.414 $\pi_{\text{forward-looking}}$		0.575 $\pi_{\text{forward-looking}}$
Fuel Usage	12932.0	13105.0	3000.0	3000.0	2031.9	3081.1
Harvest/100	120.54	120.54	41.136	28.756	30	30
Shadow price	-		$\lambda_{fuel} = 1.1705$		$\lambda_{hold} = 132.21$	
Travel%	4.2%	6.6%	16.81%	9.8%	23.47%	9.6%
Fishing%	95.8%	93.4%	83.2%	90.2%	76.5%	90.4%
Trip Length (day)	55.031	56.468	13.647	13.147	9.5919	13.485

<sup>1</sup> Travel% denotes percentage of travel time of the total trip length. Same for Fishing%.

### Appendix E.3. Results for different catch-effort elasticity

The set of sensitivity analysis focus on how catch-effort elasticity, denoted as  $\gamma$ , affects the fishing decisions. Given  $0 < \gamma < 1$ , harvest displays decreasing returns to scale with respect to effort. In the baseline case,  $\gamma = 0.7$  (the derived catchability  $q = 1.5920e-05$ ). To assess sensitivity, we then evaluate two additional cases: a lower elasticity with  $\gamma = 0.5$  and a higher elasticity with  $\gamma = 0.8$ . Throughout these analyses, we retain the spatial proximity of the sites and the assumption that nearshore sites possess higher stock levels.

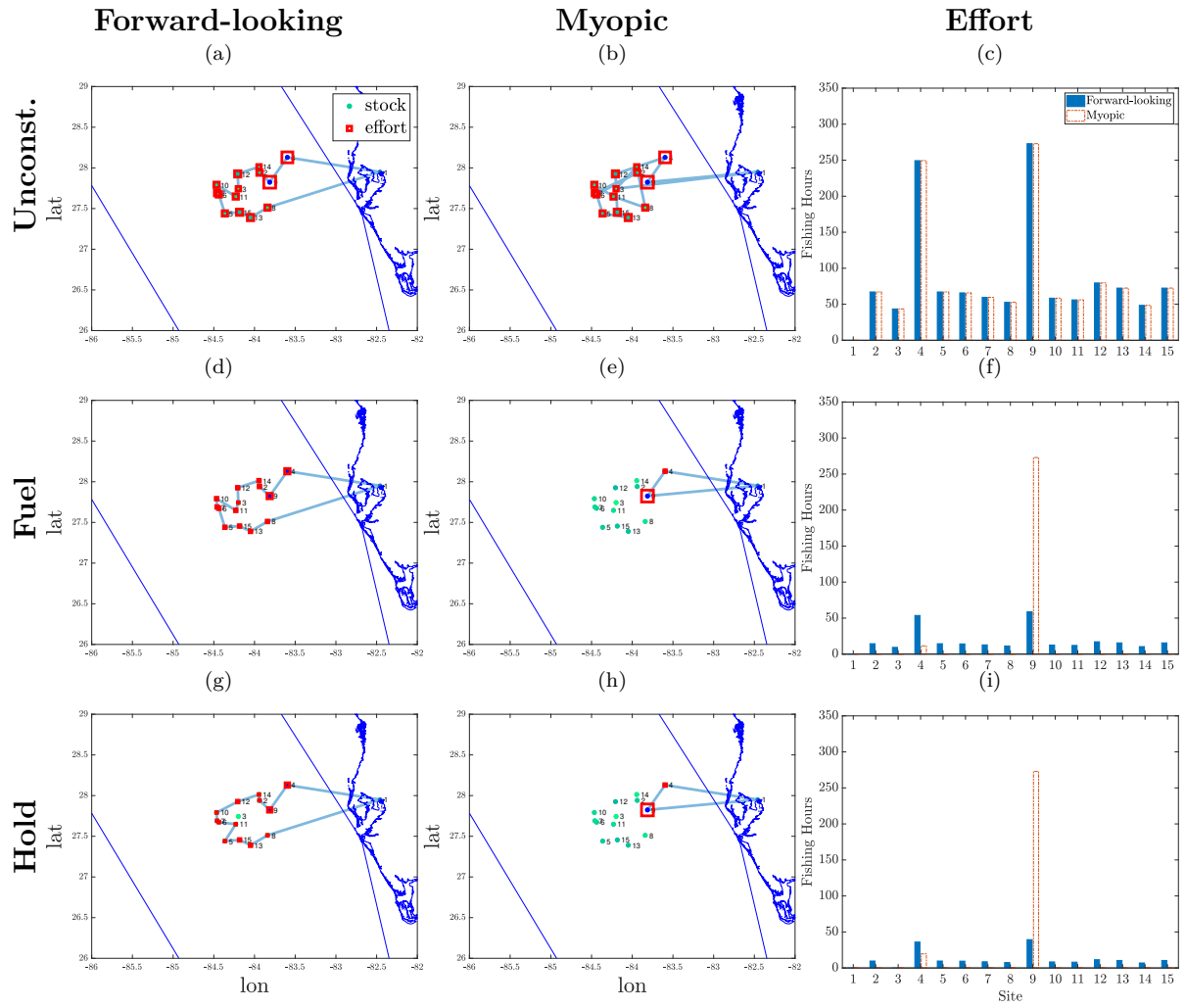


Figure E.2.2: Simulated travel path and fishing effort, forward-looking vessel vs myopic vessel, with clustered sites.

The catchability coefficient  $q$  is subject to change during the sensitivity analysis. If  $q$  remains constant and all other variables are held fixed, an increase in catch-effort elasticity,  $\gamma$ , would increase the unconstrained optimal effort. This is attributed to the principle that the unconstrained optimal effort equalizes marginal profit to zero. For the marginal revenue to stay consistent with an unchanged fishing cost, the term  $\gamma \times A_i^{\gamma-1}$  must be invariant. Consequently, when  $\gamma$  increases,  $A_i^{\gamma-1}$  should diminish. As  $\gamma - 1$  becomes a smaller negative value, the fishing hour  $A_i$  should increase to reduce the magnitude of  $A_i^{\gamma-1}$ . Nonetheless, there exists a scenario where an elevation in  $\gamma$  and  $q$  unchanged results in an unconstrained optimal effort that exceeds the available stock, necessitating an adjustment in  $q$  corresponding to changes in  $\gamma$ . When  $q$  varies with  $\gamma$ , with all other factors remaining equal, an increase in catch-effort elasticity,  $\gamma$  would instigate a decrease in both catchability  $q$  and the unconstrained optimal effort.

#### *Appendix E.3.1. Lower catch-effort elasticity $\gamma = 0.5$*

Results are summarized in Table E.3.1.1 and Figure E.3.1.1. In this examination, we adjust the catch-effort elasticity  $\gamma$  to a value of 0.5, lower than the baseline value of 0.7. This adjustment suggests that, holding other factors constant, an incremental increase in effort yields a comparatively smaller harvest at  $\gamma = 0.5$  than at  $\gamma = 0.7$ . Accompanying this decrease in  $\gamma$  to 0.5 is an increase in the derived value of catchability  $q$  ( $q = 3.6298e - 04$ ). Consequently, this prompts a rise in the unconstrained optimal effort that drives the marginal profit to zero, and results in increased optimal harvest levels across sites. Because of the escalation in effort and harvest, we set the sufficiently large fuel capacity  $F_{max} = 200,000$  and hold capacity  $C_{max} = 200,000$  to ensure the technology constraint is non-binding.

When the fuel constraint is binding, the fishing and traveling time are the same as the baseline case of  $\gamma = 0.7$  for the forward-looking vessel. Nonetheless, a notable distinction arises due to the elevated catchability coefficient at  $\gamma = 0.5$ : fishing efforts are more evenly distributed across sites. Specifically, efforts at nearshore sites with higher stock decrease

while efforts at offshore sites with lower stock increase. Given the same fuel and fishing time allocation, this leads to an increase in catch and profits for the forward-looking vessel, widening the profit disparity between the forward-looking and the myopic vessels.

However, when the hold constraint is binding, the forward-looking vessel predominantly operates in near-shore sites. Interestingly, this narrows the profit gap between the forward-looking and the myopic vessel.

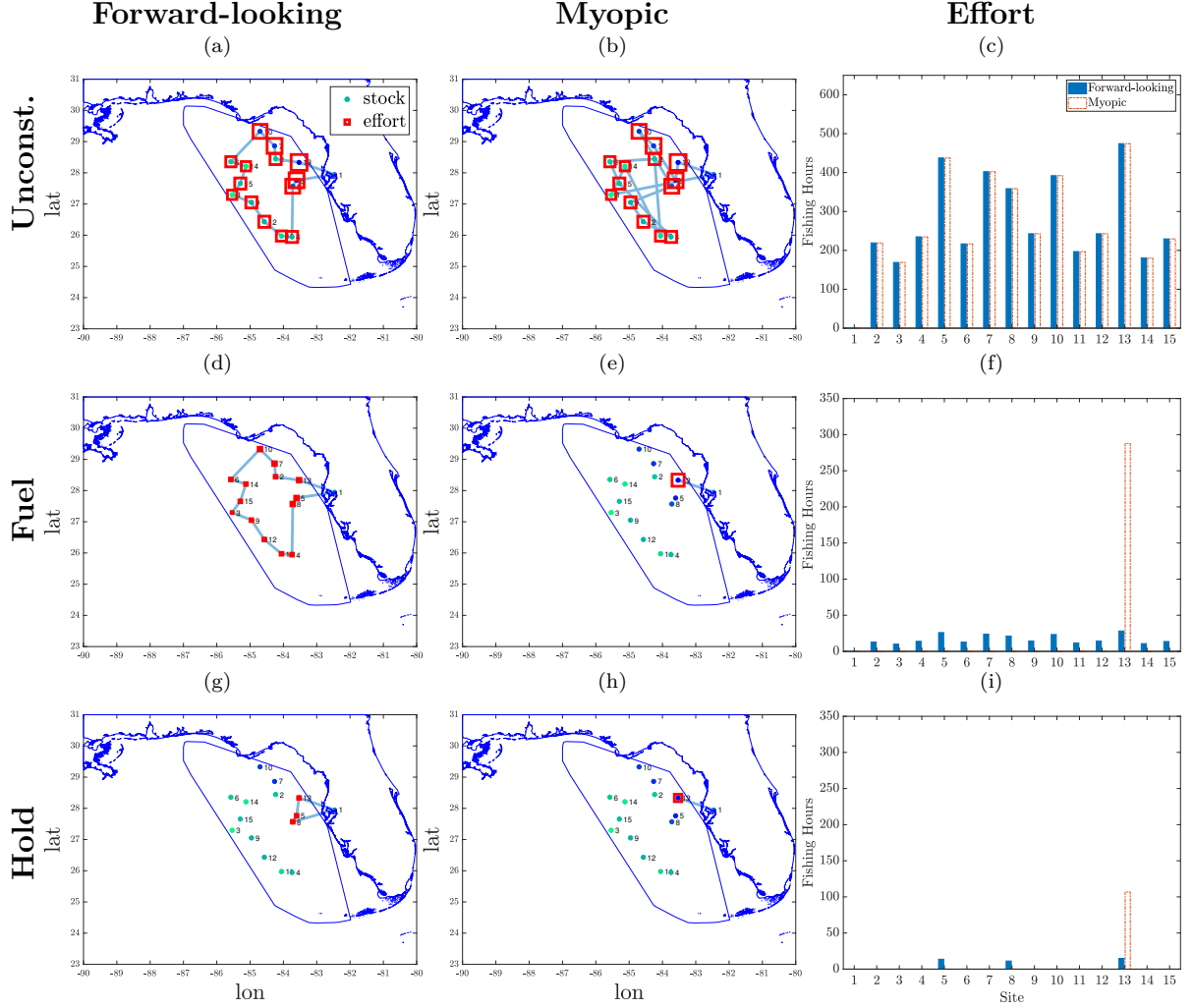


Figure E.3.1.1: Simulated travel path and fishing effort, forward-looking vessel vs myopic vessel, with catch-effort elasticity  $\gamma = 0.5$ .

Table E.3.1.1: Fuel and Hold Usage, Binding Constraints, Shadow Price, Travel Route and Time with  $\gamma = 0.5$

Variable	Unconstrained		Fuel		Hold	
	$F_{max} = 200,000, C_{max} = 200,000$	$F_{max} = 3,000, C_{max} = 200,000$	$F_{max} = 3,000, C_{max} = 200,000$	$F_{max} = 200,000, C_{max} = 3,000$	$F_{max} = 200,000, C_{max} = 3,000$	$F_{max} = 200,000, C_{max} = 3,000$
Vessel Type	Forward-looking	Myopic	Forward-looking	Myopic	Forward-looking	Myopic
Profit	0.98378 $\pi_{\text{forward-looking}}$		0.26627 $\pi_{\text{forward-looking}}$		0.84386 $\pi_{\text{forward-looking}}$	
Fuel Usage	40598.0	41236.0	3000.0	3000.0	578.12	1190.5
Harvest/100	532.96	532.96	129.89	49.261	30.0	30.0
Shadow price	-		$\lambda_{\text{fuel}} = 6.2062$		$\lambda_{\text{hold}} = 246.88$	
Travel%	3.04%	5.95%	34.5%	7.85%	47.43%	18.7%
Fishing%	96.96%	94.05%	65.5%	92.2%	52.57%	81.34%
Trip Length (day)	171.77	177.08	15.107	13.011	3.1577	5.4708

<sup>1</sup> Travel% denotes the percentage of travel time of the total trip length. Same for Fishing%.

### Appendix E.3.2. Higher catch-effort elasticity $\gamma = 0.8$

Results are summarized in Table E.3.2.1 and Figure E.3.2.1. Considering  $\gamma = 0.8$ , which is greater than 0.7. This implies that an additional unit of effort will produce relatively more harvest than it would at  $\gamma = 0.7$ , holding others constant. With  $\gamma$  increases to 0.8, the derived value of catchability  $q$  diminishes ( $q = 3.2593e - 06$ ). This leads to a reduction in the unconstrained optimal effort, which equalizes the marginal profit to zero. As a consequence, both the unconstrained optimal harvest and the fishing profit at each site decline. Meanwhile, the travel costs remain constant. For offshore sites with comparatively less stock, the fishing profits are insufficient to offset the travel cost incurred from transitioning from nearshore sites. Therefore, even in the unconstrained case, the forward-looking fisher targets only the nearshore sites with abundant stock. In contrast, the myopic vessel which does not account for travel costs explores all sites in the unconstrained case.

However, we also see less difference between the forward-looking and myopic fishers when technology constraints are binding. This convergence can be attributed to the decreased effort level which subsequently reduces the inefficiencies inherent in the strategies for the myopic fisher.

Given the baseline constraints (fuel capacity  $F_{max} = 20,000$  gallons, hold capacity  $C_{max} = 3,000$  lbs), both the forward-looking vessel and the myopic vessel retain some unused hold capacity. For the forward-looking vessel, the total unconstrained harvest does

not surpass the 3,000 lbs limit. For the myopic vessel, limited fuel restricts further travel and fishing beyond the nearshore sites. The unconstrained total harvest which drives the marginal profit of effort to zero at the nearshore sites does not exceed the 3,000 lbs hold capacity.

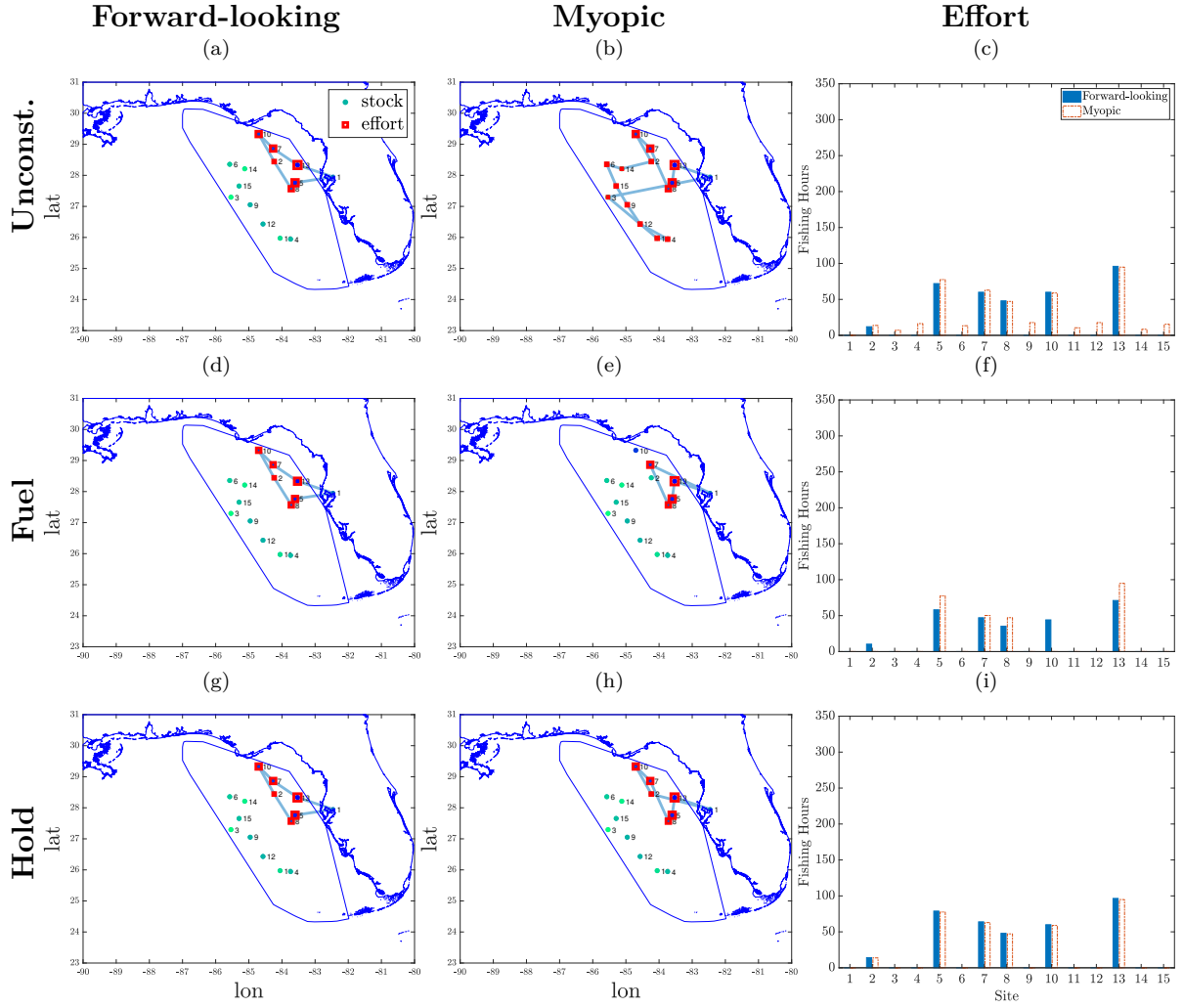


Figure E.3.2.1: Simulated travel path and fishing effort, forward-looking vessel vs myopic vessel, with catch-effort elasticity  $\gamma = 0.8$ .

Table E.3.2.1: Fuel and Hold Usage, Binding Constraints, Shadow Price, Travel Route and Time with  $\gamma = 0.8$

Variable	Unconstrained		Fuel		Hold	
	$F_{max} = 20,000, C_{max} = 20,000$	$F_{max} = 3,000, C_{max} = 20,000$	$F_{max} = 20,000, C_{max} = 3,000$	$F_{max} = 20,000, C_{max} = 3,000$	$F_{max} = 20,000, C_{max} = 3,000$	$F_{max} = 20,000, C_{max} = 3,000$
Vessel Type	Forward-looking	Myopic	Forward-looking	Myopic	Forward-looking	Myopic
Profit	0.57519 $\pi_{\text{forward-looking}}$		0.76854 $\pi_{\text{forward-looking}}$		0.91829 $\pi_{\text{forward-looking}}$	
Fuel Usage	3891.7	5460.9	3000.0	3000.0	3891.7	3936.4
Harvest/100	29.595	38.505	23.483	22.677	29.595	29.595
Shadow price	-		$\lambda_{fuel} = 0.11906$		$\lambda_{hold} = 0$	
Travel%	16.08%	26.67%	20.38%	18.28%	16.08%	17.82%
Fishing%	83.92%	73.33%	79.62%	81.72%	83.92%	82.18%
Trip Length (day)	17.633	26.255	13.918	13.757	17.633	18.006

<sup>1</sup> Travel% denotes the percentage of travel time of the total trip length. Same for Fishing%.

## Appendix F. Equivalence of the binding constraints

In this appendix, we aim to demonstrate the equivalence within a deterministic framework (no uncertainty in catch or fuel consumption): the outcomes derived from a binding fuel constraint along with a positive shadow price of fuel can be equated to those from a binding hold constraint along with a positive shadow price of hold. While the two shadow prices may differ in value, they produce identical sets of results.

Suppose fuel constraint binds for the fisher, a nonzero shadow price of fuel  $\lambda_{fuel}^*$  affects the decision-making on location choice, fishing effort, and travel path. There is a corresponding binding hold constraint and nonzero shadow price of hold  $\lambda_{hold}^*$  that leads to the same set of location choice, fishing effort, and travel path.

The relationship between  $\lambda_{hold}^*$  and  $\lambda_{fuel}^*$  can be derived from the first-order condition of fishing effort at each site.

$$\begin{aligned}\partial \mathcal{L} / \partial A_i &= pq \text{Stock}_i y_i \gamma A_i^{\gamma-1} \eta^\gamma - c_{fuel} a f \eta \kappa - \lambda_{fuel} a f \eta \kappa - \lambda_{hold} q \text{Stock}_i y_i \gamma A_i^{\gamma-1} \eta^\gamma = 0 \\ &= pq \text{Stock}_i y_i \gamma A_i^{\gamma-1} \eta^\gamma - c_{fuel} a f \eta \kappa = \lambda_{fuel} a f \eta \kappa + \lambda_{hold} q \text{Stock}_i y_i \gamma A_i^{\gamma-1} \eta^\gamma.\end{aligned}\tag{F.1}$$

So when the fuel constraint binds,  $\lambda_{fuel}^* > 0$ ,  $\lambda_{hold} = 0$ , the corresponding  $\lambda_{hold}^*$  that produces the same set of results as the given  $\lambda_{fuel}^*$  will be:

$$\begin{aligned} \lambda_{hold}^* q \text{Stock}_i y_i \gamma A_i^{\gamma-1} \eta^\gamma &= \lambda_{fuel}^* a f \eta \kappa, \\ \Rightarrow \lambda_{hold}^* &= \frac{\lambda_{fuel}^* a f \eta \kappa}{q \text{Stock}_i y_i \gamma A_i^{\gamma-1} \eta^\gamma} \end{aligned} \quad (\text{F.2})$$

Vice versa, if the hold constraint binds, the corresponding  $\lambda_{fuel}^*$  with given  $\lambda_{hold}^*$  will be:

$$\begin{aligned} \lambda_{fuel}^* a f \eta \kappa &= \lambda_{hold}^* q \text{Stock}_i y_i \gamma A_i^{\gamma-1} \eta^\gamma, \\ \Rightarrow \lambda_{fuel}^* &= \frac{\lambda_{hold}^* q \text{Stock}_i y_i \gamma A_i^{\gamma-1} \eta^\gamma}{a f \eta \kappa} \end{aligned} \quad (\text{F.3})$$

For example, when the fuel constraint binds for a vessel with fuel capacity with  $F_{max} = 3000$ , the shadow price of fuel is  $\lambda_{fuel}^* = 1.6031$  under the current parameterization. The corresponding shadow price of hold capacity will be  $\lambda_{hold}^* = 133.4766$  where the hold constraint would bind with hold capacity  $C_{max} = 40.7374$ .

## Appendix G. Impacts of fuel tax on myopic vessels

Table G.1: Fuel tax impacts on myopic vessels

Tax/Fuel capacity	Fuel reduction %			Profit reduction %			Site counts		
	Small	Medium	Large	Small	Medium	Large	Small	Medium	Large
0	-	-	-	-	-	-	1	2	3
0.25	0	0	0	21.08	-1.89	40.4	1	2	4
0.5	0	0	0	42.16	-3.79	14.66	1	3	7
0.75	0	0	1.48	63.24	4.69	15.09	1	4	11
1	0	0	12.84	84.33	13.62	40.79	1	5	14
1.5	100	0	42.42	100	57.69	80.88	0	12	14
2	100	100	100	100	100	100	0	0	0
$\lambda_{fuel}$ pre-tax last site	3.7579	2.1204	0.4153						

<sup>1</sup> Both fuel consumption and profit are compared to the pre-tax baseline value to calculate percentage reductions.

<sup>2</sup> Small/Medium/Large refers to fuel capacity  $F_{max} = 200/3000/6000$ .